doi:10.1093/brain/aws254 Brain 2012: 135; 3355–3370 | 3355

BRAIN
A JOURNAL OF NEUROLOGY

Inhibition of rho kinase enhances survival of dopaminergic neurons and attenuates axonal loss in a mouse model of Parkinson's disease

Lars Tönges,[1,*] Tobias Frank,[1,*] Lars Tatenhorst,[1,*] Kim A. Saal,[1] Jan C. Koch,[1] Éva M. Szegő,[2,3] Mathias Bähr,[1,2] Jochen H. Weishaupt[4] and Paul Lingor[1,2]

1 Department of Neurology, University Medicine Göttingen, 37075 Göttingen, Germany
2 Cluster of Excellence, Nanoscale Microscopy and Molecular Physiology of the Brain (CNMPB), 37075 Göttingen, Germany
3 Department of Neurodegeneration and Restorative Research, University of Göttingen, 37075 Göttingen, Germany
4 Department of Neurology, Ulm University, 89081 Ulm, Germany

*These authors contributed equally to this work.

Correspondence to: Lars Tönges,
Department of Neurology,
University Medicine Göttingen,
Robert-Koch-Str. 40,
37075 Göttingen, Germany
E-mail: ltoenge@gwdg.de

Correspondence may also be addressed to: Paul Lingor
Department of Neurology, University Medicine Göttingen, Robert-Koch-Str. 40, 37075 Göttingen, Germany, E-mail: plingor@gwdg.de

Axonal degeneration is one of the earliest features of Parkinson's disease pathology, which is followed by neuronal death in the substantia nigra and other parts of the brain. Inhibition of axonal degeneration combined with cellular neuroprotection therefore seem key to targeting an early stage in Parkinson's disease progression. Based on our previous studies in traumatic and neurodegenerative disease models, we have identified rho kinase as a molecular target that can be manipulated to disinhibit axonal regeneration and improve survival of lesioned central nervous system neurons. In this study, we examined the neuroprotective potential of pharmacological rho kinase inhibition mediated by fasudil in the *in vitro* 1-methyl-4-phenylpyridinium cell culture model and in the subchronic *in vivo* 1-methyl-4-phenyl-1,2,3,6-tetrahydropyridine mouse model of Parkinson's disease. Application of fasudil resulted in a significant attenuation of dopaminergic cell loss in both paradigms. Furthermore, dopaminergic terminals were preserved as demonstrated by analysis of neurite network *in vitro*, striatal fibre density and by neurochemical analysis of the levels of dopamine and its metabolites in the striatum. Behavioural tests demonstrated a clear improvement in motor performance after fasudil treatment. The Akt survival pathway was identified as an important molecular mediator for neuroprotective effects of rho kinase inhibition in our paradigm. We conclude that inhibition of rho kinase using the clinically approved small molecule inhibitor fasudil may be a promising new therapeutic strategy for Parkinson's disease.

Keywords: axonal degeneration; dopaminergic cell death; rho kinase; Parkinson's disease; 1-methyl-4-phenyl-1,2,3,6-tetrahydropyridine

Abbreviations: DOPAC = dihydroxyphenylacetic acid; HPLC = high-performance liquid chromatography; MAPK = mitogen-activated protein kinase; MPP^+ = 1-methyl-4-phenylpyridinium; MPTP = 1-methyl-4-phenyl-1,2,3,6-tetrahydropyridine; MTT = 3-(4,5-dimethylthiazol-2-yl)-2,5-diphenyltetrazoliumbromide; STAT = signal transducer and activator of transcription

Received July 11, 2012. Revised July 18, 2012. Accepted July 21, 2012

Introduction

Parkinson's disease is the most common neurodegenerative movement disorder with a median age of onset of ~55 years and a prevalence of 3% in people >80 years (Strickland and Bertoni, 2004). The disorder is commonly diagnosed by its motor symptoms, but non-motor symptoms occur even before the onset of motor deficits and represent a major therapeutic problem (Lingor *et al.*, 2011). All therapeutic approaches that are in clinical use today treat the symptoms, and there is an urgent need for the development of therapies that target the pathogenic mechanisms and act in a neuro-restorative manner (reviewed in Lees *et al.*, 2009).

While the preferential loss of dopaminergic neurons in the substantia nigra pars compacta and the presence of Lewy bodies are considered as hallmarks of the disease (Braak *et al.*, 2003), its initial pathology is likely to be characterized by neuritic and axonal degeneration (reviewed in Burke and O'Malley, 2012). Although Bernheimer *et al*. (1973) described that at the time of clinical diagnosis in human patients, ~60% of substantia nigra pars compacta neurons have been lost and ~80% of dopaminergic terminals are dysfunctional (Bernheimer *et al.*, 1973), a recent comprehensive analysis of the literature suggests that the initial degeneration of the striatal innervation seems to be much more prominent. Burke and O'Malley (2012) conclude that at the time when first motor signs appear, there is only ~30% loss of total substantia nigra pars compacta neurons, which is by far exceeded by the loss of striatal or putamenal dopaminergic markers that is estimated to be ~70–80%. Thus, the extent of terminal loss in the striatum seems to be much more extensive than the amount of loss of substantia nigra pars compacta dopaminergic neurons, suggesting that the striatal dopaminergic nerve terminals are the primary target of the degenerative process and that neuronal death in Parkinson's disease represents a 'dying back' pathology (Dauer and Przedborski, 2003). This hypothesis is also supported by neuropathological findings demonstrating that Lewy neurites outnumber Lewy bodies in early-stage Parkinson's disease brains (Braak *et al.*, 2003). Additionally, there is a vast body of evidence from genetic studies of Parkinson's disease pointing to severe axonal pathology in this disease. For example, the greatest abundance of α-synuclein aggregates has been detected not in the cell bodies, but in the neuropil of human Lewy body disease brains, where it is entrapped within presynaptic terminals (Kramer and Schulz-Schaeffer, 2007). As demonstrated in a primary neuronal culture, exogenous recombinant α-synuclein fibrils can be taken up and form aggregates in the presynaptic terminal with subsequent propagation to the neuronal soma (Volpicelli-Daley *et al.*, 2011). This axon-accentuated pathology is also seen in mouse models harbouring mutations of leucine-rich repeat kinase 2 (LRRK2), a protein that is frequently mutated in inherited forms of Parkinson's disease (Greggio and Cookson, 2009).

To recapitulate Parkinson's disease in animal models, several genetic and toxin-based disease paradigms have been developed. The 1-methyl-4-phenyl-1,2,3,6-tetrahydropyridine (MPTP)-based mouse model of Parkinson's disease has been studied for >20 years and is therefore well characterized in mice and monkeys (Langston *et al.*, 1983; Cannon and Greenamyre, 2010). Using this model, several studies have clearly demonstrated cellular neuroprotective effects on dopaminergic cells with compounds such as monoamine oxidase B inhibitors, vitamin E, the mixed lineage kinase inhibitor CEP-1347, the anti-excitotoxic agent riluzole or coenzyme Q10 (Perry *et al.*, 1985; Benazzouz *et al.*, 1995; Beal *et al.*, 1998; Saporito *et al.*, 1999; Andringa *et al.*, 2003). However, these findings were never successfully translated into the clinic (Lang, 2006; Olanow *et al.*, 2006; Storch *et al.*, 2007). This may be due to the fact that these experimental approaches have not adequately focused on prevention or restoration of axonal pathology in Parkinson's disease, which is at least as important for the development of clinical disease as is the cellular damage of substantia nigra pars compacta neurons (Burke, 2010; Cheng *et al.*, 2010). Interestingly, the MPTP model is an excellent tool for the study of axonal degeneration. Already within the first days after MPTP application, the number of tyrosine hydroxylase-immunoreactive fibres in the median forebrain bundle significantly decreases, whereas the dopaminergic neuron demise follows later (Li *et al.*, 2009). In an elaborate study analysing synaptosomal preparations of MPTP-treated mice, chronically administered MPTP readily decreased the expression of the dopamine transporter at a time when cell bodies still remained intact (Muroyama *et al.*, 2011). Remarkably, MPTP-lesioned monkeys exhibit a destruction of striatal terminals preceding the loss of substantia nigra pars compacta neurons (Herkenham *et al.*, 1991), and the protection of striatal terminals alleviates the loss of substantia nigra pars compacta dopaminergic cells (Wu *et al.*, 2003). The functionality of the nigrostriatal pathway depends both on cellular and axonal integrity, but these two compartments may suffer from mechanistically different types of degeneration as it is also the case in models of Wallerian degeneration (Coleman and Perry, 2002; Raff *et al.*, 2002). Even more importantly, axonal degeneration may even precede and sometimes cause neuronal cell death (Coleman, 2005). In this study, we have examined a novel molecular target in Parkinson's disease pathology that has been involved in the regulation of both cellular and axonal demise in neurodegenerative disease models.

The enzyme rho kinase has shown to be widely distributed in the mammalian CNS, with increasing expression with age (Hashimoto *et al.*, 1999; Komagome *et al.*, 2000). It is crucially responsible for the lack of axonal regeneration in the CNS (Mueller *et al.*, 2005; Tonges *et al.*, 2011*b*). Evaluating the role of rho kinase signalling in optic nerve lesion models, we have found that pharmacological inhibition of rho kinase is able to significantly enhance regeneration of optic nerve axons after lesion. Interestingly, rho kinase inhibition has also yielded cellular neuroprotective effects and has prevented apoptosis of retinal ganglion cells after optic nerve axotomy (Lingor *et al.*, 2007, 2008). Because of these multifaceted axonal and cellular protective actions mediated by rho kinase inhibition, we have now examined the effects of the small molecule rho kinase inhibitor fasudil in the MPTP model of Parkinson's disease. Fasudil has been extensively studied in animal models of cardiovascular disease due to its additional vasodilatator and anti-arteriosclerotic effects and is being evaluated currently for its clinical applicability in this context (Loirand and Pacaud, 2010).

Having detected a protective effect on perikaryal survival and neurite stability after fasudil treatment of primary midbrain neurons subjected to the MPTP metabolite 1-methyl-4-phenylpyridinium (MPP^+) *in vitro*, we transferred these findings to the subchronic MPTP mouse model *in vivo*. Here, we were able to reproduce the neuroprotective response of pharmacological rho kinase inhibition with orally applied fasudil. The examination of neuroprotective pathways revealed an increased activation of Akt signalling after rho kinase inhibition, thus attributing rho kinase an important role in the regulation of both perikaryal survival and axonal integrity in the MPTP model of Parkinson's disease.

Materials and methods

In vitro assays of dopaminergic cell survival and of neurite regeneration

Primary midbrain dopaminergic neurons were prepared under serum-free conditions as described previously (Lingor *et al.*, 1999). Briefly, embryonic rat midbrain neurons from embryonic Day 14 Wistar rats were dissected and seeded on poly-L-ornithine/laminin-coated cover slips. On *in vitro* Days 1 and 3, cells received a treatment with phosphate buffered saline (PBS) that served as control or with different final concentrations of fasudil (4, 20 or 100 μM). Fasudil was purchased from LC Laboratories as a monohydrochloride salt [$C_{14}H_{17}N_3O_2S.HCl$; IUPAC name: 5-(1,4-diazepane-1-sulphonyl)isoquinoline], which is soluble in water. It has an half maximal inhibitory concentration (IC50) of 1.9 μM for the isoform 2 of rho kinase, which is predominantly present in the CNS (Tonges *et al.*, 2011*b*).

To evaluate cell survival, MPP^+ (Sigma) was added to the culture on *in vitro* Day 3 at a final concentration of 20 μM for 48 h. Survival of dopaminergic neurons was assessed after cell fixation and immunocytochemical processing by counting of tyrosine hydroxylase-positive immunostained cells in four randomly distributed visual fields of each cell culture. Additionally, the length of all tyrosine hydroxylase-immunopositive neurites of at least two randomly distributed visual fields of each cell culture was measured with ImageJ software to obtain the cumulative neurite length per visual field. This value was then divided by the number of tyrosine hydroxylase-positive cells per visual field to calculate neurite length per cell.

Neurite regeneration was evaluated with the cell scratch paradigm as described previously (Tonges *et al.*, 2011*a*). On *in vitro* Days 1 and 3, cells were treated in the same manner as for cell survival studies with PBS control or with fasudil in different final concentrations (4, 20 or 100 μM). Neurite processes were mechanically transected with a thin silicone scraper on *in vitro* Day 3 and directly thereafter were treated with either PBS or MPP^+ (final concentration 20 μM). After 48 h, cells were fixed, and the culture was immunolabelled for tyrosine hydroxylase. The length of the 10 longest tyrosine hydroxylase-immunopositive neurites from the scratch border was measured with ImageJ software in at least three randomly distributed visual fields of each cell culture.

Immunocytochemistry

For visualization of dopaminergic neurons, cells were fixed in 4% paraformaldehyde for 10 min at room temperature (22°C), permeabilized with 100% ice-cold acetone (AppliChem) for 10 min at −20°C, washed twice with PBS and blocked with 10% normal goat serum for 10 min at room temperature. Probes were incubated with the primary antibodies [rabbit anti-tyrosine hydroxylase 1:250 (Zytomed)] overnight at 4°C. After two washes with PBS, the appropriate Cy3-labelled secondary antibody (1:250, Dianova) was applied for 45 min at 37°C. Cell nuclei were then counter-stained with 4,6-diamidino-2-phenylindole (DAPI; Sigma) and mounted in Mowiol® (Hoechst). Fluorescence was observed and recorded on a Zeiss Axioplan-2 fluorescence microscope equipped with a CCD camera and AxioVision software (Carl Zeiss MicroImaging). For evaluation of dopaminergic survival and measurement of the neurites within the culture, pictures of two to four random visual fields per culture well were taken with a ×20 objective. For evaluation of dopaminergic regeneration at the scratch site, pictures of three random visual fields at the scratch site were taken with a ×20 objective.

Western blots

To study the activation of cell survival pathways in midbrain dopaminergic neurons, cells were treated as described before for the *in vitro* assay of cell survival. 48 hours after MPP^+ application, cells were lysed with a cell lysis buffer consisting of 10 mM HEPES (pH 7.2), 142 mM KCl, 5 mM $MgCl_2$, 1 mM EGTA and 1% IGEPAL® plus protease inhibitors ('Complete tablets', Roche). The protein content of all cell samples was determined using the Bradford assay (Biorad), and equal amounts of protein (50 μg) were separated on a sodium dodecyl sulfate polyacrylamide gel electrophoresis (SDS-PAGE). Proteins were then electrotransferred onto a nitrocellulose membrane and blocked with 5% bovine serum albumin in Tris-buffered saline/Tween 20 (TBS-T) for 1 h. Membranes were then incubated with primary antibodies (anti-phosphorylated STAT3, anti-STAT3, anti-phosphorylated Akt, anti-Akt, anti-phosphorylated MAPK, anti-MAPK, anti-Bcl2, all 1:1000; all Cell Signaling Technologies; anti-growth associated protein-43 (GAP43), 1:100, Abcam) for 24 h at 4°C in TBS-T and 2% bovine serum albumin or with anti-GAPDH (1:5000, Biotrend) for 1 h at room temperature in TBS-T and 5% bovine serum albumin. This was followed by incubation with corresponding horseradish peroxidase-coupled secondary antibodies (1:1000 for 1 h at room temperature; Dianova). ECL Plus™ reagent (Amersham) was applied on the membrane, and the chemiluminescence was visualized on X-ray films (Kodak).

Subchronic MPTP mouse model of Parkinson's disease and treatment with fasudil

For experiments with MPTP, 8- to 10-week-old male mice (C57BL/rehydration and 6JOla Hsd) were purchased from Harlan Winkelmann. Animals (n = 5–8 per experimental group) were housed in groups of five in individually ventilated cages (IVC, Tecniplast). They were kept under a 12-h light/12-h dark cycle with free access to food and water. For MPTP intoxication, mice received a total of five intraperitoneal injections of 30 mg/kg body weight MPTP (free base) dissolved in 0.9% saline on five consecutive days. The control group was injected with saline only. Appropriate guidelines were followed in handling MPTP and MPTP-injected mice (Przedborski *et al.*, 2001). Fasudil was given at 100 mg/kg body weight as per oral gavage by feeding tubes for 2 weeks in the short treatment regimen. In the 6-week treatment period, it was applied at 30 mg or 100 mg/kg body weight in drinking water. The drinking behaviour was closely monitored to ensure an adequate dosage of fasudil. Treatment was started one day before the first MPTP application in the 2-week experiment, and it was started on the day of the first MPTP application in the 6-week experiment. Treatment was continued until animals were

sacrificed 2 or 6 weeks after the first treatment application. All animal experiments were carried out according to the regulations of the local animal research council and legislation of the State of Lower Saxony.

Immunohistochemistry

Having completed the respective treatment periods, mice were sedated with chloral hydrate and perfused transcardially with saline, followed by 4% paraformaldehyde in PBS (pH 7.4). For the fasudil-treated animals treated for 2 weeks and the controls, the brains were quickly dissected, post-fixed in paraformaldehyde overnight at 4°C, cryoprotected in 30% sucrose in PBS for 24 h at 4°C, snap frozen and stored at −80°C until sectioning. For each group, frontal cryosections (25 μm) through the entire striatum and the substantia nigra were collected on object slides. After rehydration and several rinses in PBS, sections were blocked in 10% normal goat serum for 30 min at room temperature. This was followed by incubation with a polyclonal anti-tyrosine hydroxylase antibody (1:1000; RH-TH-15; Zytomed) or anti-NeuN antibody (1:1000; MAB377; Millipore) diluted in 0.1% Triton® X-100 and 1% normal goat serum in PBS for 24 h at 4°C. All brains were processed with the same antibody lot. After three rinses in PBS, sections were incubated with Cy3- or Cy2-conjugated affinity-purified IgG (goat-anti-rabbit; 1:200; Dianova) for 1 h at room temperature. Finally, sections were DAPI stained and mounted.

For fasudil-treated animals treated for 6 weeks and controls, brains were cryosectioned (30 μm) as described above and were then kept in 0.1% sodium azide. Using a free-floating method, sections were rinsed in 0.1 M Tris-buffered saline (pH 7.4) followed by a treatment with 10% methanol and 3% H_2O_2 in Tris-buffered saline for 5 min, then rinsed again three times in Tris-buffered saline and blocked with 5% normal goat serum in Tris-buffered saline for 60 min. Sections were incubated with a polyclonal anti-tyrosine hydroxylase antibody (1:1000; Chemicon) in 1% normal goat serum for 48 h and 4°C. After three rinses in Tris-buffered saline, the sections were treated with a secondary biotinylated antibody (1:200, Dianova) in Tris-buffered saline at room temperature for 60 min followed by rinsing in Tris-buffered saline again and incubation with VECTASTAIN® ABC Peroxidase (Standard Kit, PK-4000, Biozol) for 60 min at room temperature. After rinsing in Tris-buffered saline, the sections were treated with 3,3′-diaminobenzidine (DAB peroxidase substrate Kit, SK-4100, Vector Laboratories) for 4 min, rinsed again and collected on object slides. Having dried for ∼4 days, sections were dehydrated, and a Nissl staining procedure was performed by rinsing sections in water for 5 min, followed by an incubation in 1% thionine acetate (Sigma) for 7 min. Sections were rinsed with water again for 5 min, followed by a dehydration row with 70, 90 and 95% ethanol each for 5 min, followed by 5 min in 100% isopropanol and subsequent incubation at least three times in Xylol for 5 min. Finally, sections were mounted with DPX (Fluka Chemica).

For staining of striatal tyrosine hydroxylase-positive fibres, slices were incubated in chloroform–ethanol followed by dehydration, use of anti-tyrosine hydroxylase antibody (Zytomed) and DAB staining (Elite ABC Kit, Vector Laboratories), nickel intensification, formalin fixation and dehydration. Entellan® was used to mount the sections. Details are given in Schulz *et al.* (1995).

Stereological quantification of substantia nigra neurons and evaluation of striatal density

The number of tyrosine hydroxylase-, NeuN- or Nissl-positive cells in the substantia nigra was assessed using stereological methodology. Every fourth section through the substantia nigra was analysed using Stereo Investigator software (Stereo Investigator 9.0, MicroBrightField Inc.) and a Zeiss Axioplan microscope (Dehmer *et al.*, 2004). A point grid was overlaid onto each section including the substantia nigra pars compacta only. Immunostained cells were counted by the optical fractionator method (×40 objective, counting frame 50 × 50 μm). The evaluation of NeuN and Nissl cells was performed to confirm loss of neurons rather than merely down-regulation of the tyrosine hydroxylase enzyme. Stereological counts were performed by a blinded investigator. Values represent one substantia nigra per animal.

Tyrosine hydroxylase-positive fibre density in the striatum was assessed in sections between Bregma +0.62 and −0.10 mm slightly modified from a previously published protocol (Szego *et al.*, 2012). Every fourth striatal section was immunolabelled for tyrosine hydroxylase resulting in a total of six sections that were analysed per animal. In every section, four to six images were taken using a ×100 objective (Zeiss Axioplan) followed by image processing with background subtraction and binarization to optimally visualize tyrosine hydroxylase-immunopositive fibre areas. These were quantified as percentage of total area at 10 randomly distributed sites from the same image (ImageJ 1.43 u).

Neurochemical analysis of dopamine and metabolites

Twelve days after the first MPTP injection, animals were sacrificed and striata ($n = 8$ per experimental group) were immediately dissected on ice. Tissue samples were homogenized in a bead mill homogenizer (Precellys 24®, Peqlab) with 50 μl of 0.1 M perchloric acid per mg of striatal tissue. After centrifugation (5000*g* for 1 min followed by 10 000 *g* for 30 min, 4°C), 50 μl of supernatant was injected onto a C18 reverse-phase HR-80 catecholamine column (ESA). Dopamine, 3,4-dihydroxyphenylacetic acid and homovanillic acid were quantified by high-performance liquid chromatography (HPLC) with electrochemical detection. The mobile phase (pH = 2.9) consisted of 90% 75 mM sodium phosphate, 275 mg/l octane sulphonic acid solution and 10% methanol. Flow rate was 0.8 ml/min. Peaks were detected by an ESA Coulochem II with a model 5010 detector (E1 = 20 mV, E2 = 320 mV). Data were collected and processed using the Chromeleon computer system (Dionex).

MPTP metabolism

MPP^+ levels in the brain were determined by HPLC modified from the method described by Przedborski *et al.* (1996). Four mice of each experimental group were orally fed with either 100 mg/kg fasudil or the same volume of buffer (see above). Six hours later the mice were intraperitoneally injected with 30 mg/kg MPTP (free base). Mice were sacrificed 90 min later. Striata were quickly dissected on ice and frozen at −80°C until further processing. Tissue samples were homogenized in 50 μl of 0.1 mol/l perchloric acid per milligram tissue, and the debris removed by high-speed centrifugation. Supernatant (10 μl) was injected onto a reverse-phase column (Nucleosil 100-5 C18; Macherey-Nagel) and detected by fluorescence at an excitation wavelength of 295 nm and an emission wavelength of 375 nm (Fluorescence HPLC Monitor; Shimadzu). The mobile phase consisted of 650/1000 ml acetonitrile in phosphate buffer (pH 2.5). The flow rate was 0.4 ml/min.

Behavioural analysis

The Cylinder test (Schallert *et al.*, 2000) was adapted for use in mice to assess forelimb use during normal exploratory activity and was performed 2 or 6 weeks after the initial MPTP lesion in enlarged cohorts of animals ($n = 14$–15 per experimental group). Each mouse was placed in a transparent cylinder of 11.5 cm diameter and 25 cm in height for 5 min and videotaped during the test. A mirror was arranged behind the cylinder at an angle to enable the rater to record forelimb movements when the mouse turned away from the camera. Forelimb use of the first contact against the wall after rearing and during lateral exploration was recorded by the following criteria: (i) the first forelimb to contact the wall during a full rear was recorded as an independent wall placement for that limb; (ii) simultaneous use of both the left and right forelimb by contacting the wall of the cylinder during a full rear and for lateral movements along the wall was recorded as movement with 'both' forelimbs; (iii) full rears of the entire body without touching the wall with neither left nor right forelimb were recorded as 'free' rears; and (iv) when the mouse explored the wall laterally, alternating both forelimbs, it was recorded as movement with 'both' forelimbs. All movements were recorded during the 5-min test. The statistical analysis detailed the percentage of 'both', 'right', left' or 'free' movements of all movements observed in the entire observation time.

The rotarod test was performed in the same cohorts subjected to the cylinder test 2 or 6 weeks after the initial MPTP lesion. To measure motor balance and coordination, mice were placed on a horizontal rotating rod with 3 cm diameter (rotarod for mice 47600, Ugo Basile). Five mice were tested simultaneously, separated by large disks. After the mice were placed on the rod at constant rotation speed of 5 rpm, the trial was started and rotation speed was automatically increased from 5 to 40 rpm within 5 min. The trial stopped when the mouse fell down, activating a switch that automatically stopped a timer, or when 5 min were completed. All mice were pre-trained on the rotarod on three consecutive days before MPTP treatment in order to reach a stable performance. The final test was performed in three sessions with an intertrial interval of 30 min to reduce stress and fatigue. Rotarod performance in all three runs was recorded, and the average time on the rotarod was compared between groups.

Statistical analysis

Statistical comparisons of values between two groups were carried out by unpaired Student's *t*-test, and multiple group comparisons for *in vitro* experiments were carried out by two-way ANOVA followed by Tukey's *post hoc* test. Statistical comparisons of values between two animal groups were carried out by unpaired Student's *t*-test, and multiple group comparisons in animal experiments were conducted by one-way ANOVA with Tukey's *post hoc* test. Striatal fibre density measurements were performed in a hierarchically nested design, the dependent variable being the fibre density, and the independent variables being vehicle or MPTP treatment, respectively. For statistical analyses, Kyplot software version 2.0 (KyensLab Incorporated), Statistica version 9.1 (StatSoft Inc.) and R software version 2.8.0 (R Development Core Team) were used. Data are represented as mean ± SEM or standard deviation (SD) as indicated. Significances are indicated with $*P < 0.05$; $**P < 0.01$; $***P < 0.001$, unless stated otherwise.

Results

Pharmacological rho kinase inhibition with fasudil protects midbrain dopaminergic neurons from MPP^+ toxicity *in vitro*

We first studied the cell survival-promoting effects of the rho kinase inhibitor fasudil in the MPP^+ neurotoxicity model in midbrain dopaminergic neuron cultures. Cell cultures that had only received a control treatment showed a significantly decreased number of surviving tyrosine hydroxylase-positive cells after MPP^+ application (64.7 ± 4.9%) compared with PBS treatment, which was set to 100% (100 ± 2.6%). However, cell cultures that had been treated with an optimal concentration of fasudil (20 μM) and were subjected to MPP^+ resulted in higher numbers of tyrosine hydroxylase-positive cells (85.9 ± 2.8%). A low or a high concentration of fasudil (4 and 100 μM, respectively) did not confer any cellular protection (72.3 ± 2.7% and 59.3 ± 3.0%). It is known that midbrain dopaminergic neurons that are not MPP^+ lesioned and cultured under standard serum-free conditions still suffer from relevant cell loss due to their maintenance in a dissociated state. Interestingly, under these control conditions, rho kinase inhibition with fasudil also conferred a neuroprotective effect and maintained higher numbers of tyrosine hydroxylase-positive neurons with the optimal concentration of 20 μM (111.7 ± 1.9%). High concentrations of fasudil (100 μM), however, appeared to be toxic and resulted in reduced cell numbers (72.1 ± 3.4%). The two-way ANOVA revealed no statistical interaction between fasudil and MPP^+, which indicates that the neuroprotective effects of fasudil are independent of MPP^+ treatment (Fig. 1).

In the same cultures, which had been plated in a growth permissive environment on laminin, we evaluated the integrity of the tyrosine hydroxylase-immunopositive neuritic network with and without MPP^+ stress. For this purpose, we measured tyrosine hydroxylase-positive neurites and quantified their length per cell in order to remain independent of cell survival effects. Compared with PBS control treatment, which was set to 100% (100 ± 5.5%), application of the optimal dose of 20 μM fasudil resulted in a significantly increased neurite length per cell (142.6 ± 7.8%). Interestingly, midbrain dopaminergic neurons that had been subjected to MPP^+ only showed a trend of reduced neurite length (79.7 ± 9.5%) whereas 20 μM fasudil still maintained a larger neurite length with MPP^+ (110.8 ± 8.2%) compared with the MPP^+ control (Fig. 2A and C). If cumulative neurite length in culture was measured without normalization to cell numbers, this resulted in an increased neurite length with 20 μM fasudil. Compared with PBS control treatment (100 ± 9.4%), 20 μM fasudil led to a significant increase (165.9 ± 7.5%). In midbrain dopaminergic neurons that had been subjected to MPP^+, 20 μM fasudil-treated cells obtained a cumulative outgrowth of 91.3 ± 12.1%, whereas the MPP^+ controls achieved only 55.8 ± 7.3% (Fig. 2B and C).

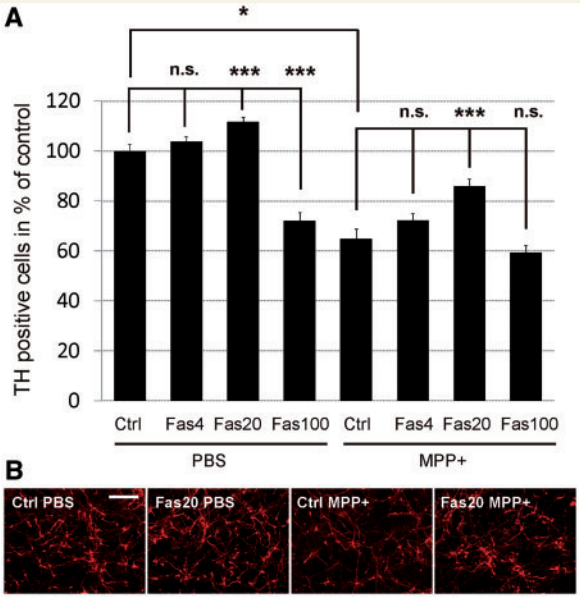

Figure 1 Survival of tyrosine hydroxylase-immunopositive neurons after 20 μM MPP^+ or PBS control treatment for 48 h. (**A**) MPP^+-treated cultures supplemented with fasudil 20 μM (Fas20) showed higher numbers of surviving tyrosine hydroxylase-immunopositive neurons compared with vehicle-treated cells (Ctrl). Bars represent means ± SEM. $^*P < 0.05$, $^{***}P < 0.001$. (**B**) Representative micrographs of midbrain dopaminergic neurons cultures labelled against tyrosine hydroxylase (Cy3, red). Scale bar = 200 μm. n.s = not significant; TH = tyrosine hydroxylase.

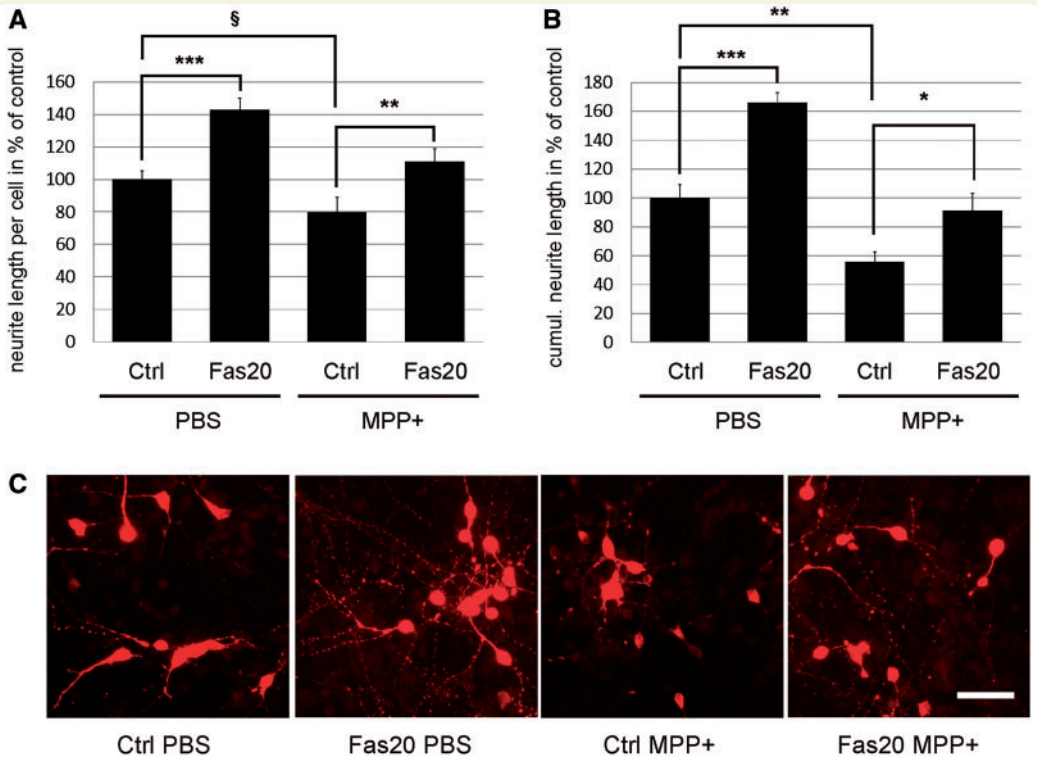

Figure 2 Quantification of tyrosine hydroxylase-immunopositive neurites 48 h after 20 μM MPP^+ or PBS control treatment. (**A** and **B**) Supplementation with fasudil 20 μM (Fas20) results in an increased neurite length per cell (**A**) and in an increased cumulative neurite length (**B**) both with and without MPP^+ stress. Bars represent means ± SEM. $^*P < 0.05$, $^{**}P < 0.01$, $^{***}P < 0.001$, $^{\S}P = 0.08$. (**C**) Representative micrographs of midbrain dopaminergic neuron cultures labelled against tyrosine hydroxylase (Cy3, red). Scale bar = 50 μm. Ctrl = control.

Dopaminergic neuronal regeneration is increased by inhibition of rho kinase

To assess the regenerative neurite outgrowth stimulatory potential of fasudil, we performed a mechanical neurite transection of midbrain dopaminergic neurons that had been cultured for 3 days. Additionally, cells were either subjected to MPP^+ or a control treatment at this time point. The evaluation of neurite outgrowth from the site of lesion was performed 2 days thereafter. Outgrowth of control-treated midbrain dopaminergic neurons was significantly reduced if cells were subjected to MPP^+ instead of a PBS control that was set to 100% (72.6 ± 7.0% versus 100.0 ± 7.3%). Whereas a cell culture supplementation with fasudil 4 μM could not improve neurite outgrowth in comparison with the respective control in both PBS- and MPP^+-treated cells (99.0 ± 4.1% and 78.0 ± 8.5%), supplementation with fasudil 20 μM was able to significantly increase the neurite length under both conditions (128.2 ± 7.5% and 101.3 ± 6.5%). The highest dose of fasudil 100 μM could improve neurite outgrowth only under PBS control conditions (134.7 ± 6.5%), but was not able to increase regeneration with concomitant MPP^+ toxicity (54.6 ± 10.5%) (Fig. 3).

Fasudil protects mouse dopaminergic neurons from MPTP toxicity

To validate the effect of rho kinase inhibition in Parkinson's disease models, we have chosen to take advantage of an *in vivo* model in which we applied MPTP in a subchronic systemic approach (MPTP injection of 30 mg/kg for five consecutive days). We found a substantial protection of tyrosine hydroxylase-immunopositive neurons in the substantia nigra 2 weeks after the first application of MPTP with daily feeding of fasudil at a dose of 100 mg/kg (7424 ± 291 cells) compared with vehicle-treated animals (5016 ± 375 cells). The non-MPTP treated control group exhibited the highest number of tyrosine hydroxylase cells (9141 ± 276 cells) (Fig. 4A and C). To verify that fasudil protection was not influenced by fasudil-dependent tyrosine hydroxylase down-regulation, we confirmed results by additional evaluation of NeuN-immunopositive cells in the substantia nigra (Fig. 4B).

The protective effect of fasudil on dopaminergic neurons was verified in a separate cohort of animals in which neuronal survival 6 weeks after the first MPTP lesioning stimulus was analysed. In this long-term treatment paradigm, both a fasudil dose of 30 mg/kg and of 100 mg/kg were applied. Compared with non-MPTP-treated controls, which exhibited highest numbers of tyrosine hydroxylase-immunopositive cells (12024 ± 1166 cells), there was no significant reduction in tyrosine hydroxylase cell numbers with MPTP treatment when fasudil was applied in both doses (fasudil 30 mg/kg: 10944 ± 522 cells; fasudil 100 mg/kg: 9755 ± 435 cells). In relation to MPTP-lesioned control animals (7949 ± 752 cells), the fasudil 30 mg/kg group showed a significantly higher number of tyrosine hydroxylase cells (Fig. 5A and C). Similar relations were found in the evaluation of Nissl-stained nigral neurons (Fig. 5B).

Fasudil prevents striatal dopamine depletion and attenuates reduction of striatal fibre density

Next, we asked whether fasudil, beyond morphological preservation of dopaminergic cell bodies, also preserves nigrostriatal innervating fibres after MPTP lesion. A 2-week treatment of fasudil (100 mg/kg) was able to significantly preserve the density of tyrosine hydroxylase-immunopositive fibres in the striatum (52.92 ± 0.89%), measured as tyrosine hydroxylase-immunopositive area in relation to the total area, in comparison with control-treated and MPTP-lesioned animals (42.72 ± 0.89%). The non-MPTP-lesioned control group exhibited the highest amount of tyrosine hydroxylase fibres (67.35 ± 0.64%) (Fig. 6A and B). To correlate striatal fibre morphology to a functional preservation of these axonal terminals, we quantified striatal dopamine and dopamine metabolite levels by HPLC. Although we found a decrease in striatal dopamine after MPTP intoxication in the vehicle groups using the same MPTP lesioning protocol as for the immunohistochemical analyses (3.56 ± 0.92 to 1.25 ± 0.18 ng/mg), dopamine levels in the fasudil and MPTP treatment group were significantly higher (2.05 ± 0.14 ng/mg) (Fig. 6C). A similar degree of preservation could be detected for homovanillic acid (vehicle control: 4.07 ± 0.65 ng/mg, MPTP control: 2.76 ± 0.46 ng/mg, fasudil MPTP: 3.96 ± 0.56 ng/mg) (Fig. 6E). Dihydroxyphenylacetic acid (DOPAC) levels were not significantly different between MPTP intoxication (13.46 ± 0.51 ng/mg) and controls (13.61 ± 0.67 ng/mg), whereas there was a trend towards higher levels in the fasudil treatment group (16.10 ± 0.95 ng/mg) (Fig. 6D). Moreover, the trend towards a lower metabolite ratio as calculated by ([homovanillic acid] + [DOPAC]) / [dopamine] in the fasudil treatment group (9.76 ± 3.14) versus MPTP control treatment (12.94 ± 3.64) indicates a reduced dopamine turnover and thus decreased cellular stress with fasudil (Fig. 6F). To exclude that fasudil by itself alters the MPTP metabolism, we measured MPP^+ levels in the striatum without detecting a significant difference among both treatment groups (MPTP control: 57.50 ± 8.89 ng/ml versus fasudil MPTP: 52.40 ± 5.00 ng/ml) (Fig. 6G).

In a separate cohort of MPTP-lesioned animals, a fasudil treatment was applied for 6 weeks in doses of 30 mg/kg and 100 mg/kg. Compared with vehicle-treated animals (67.17 ± 0.76%), the MPTP-treated animals exhibited a persistent severe reduction in the density of tyrosine hydroxylase-immunopositive fibres in the striatum (33.79 ± 0.89%). Both treatments with fasudil resulted in a significantly higher tyrosine hydroxylase fibre density compared with MPTP control-treated animals (fasudil 30 mg/kg: 48.77 ± 0.85%; fasudil 100 mg/kg: 50.56 ± 0.88%) (Fig. 7A and B). Striatal dopamine and dopamine metabolite levels showed significantly higher levels in the 30 mg/kg fasudil treatment group compared with MPTP lesioned vehicle control (dopamine: fasudil 30 mg/kg MPTP: 6.46 ± 0.81 ng/mg versus MPTP control: 3.42 ± 0.69 ng/mg; DOPAC: fasudil 30 mg/kg MPTP: 2.90 ± 0.22 ng/mg versus MPTP control: 1.90 ± 0.14 ng/mg; homovanillic acid: fasudil 30 mg/kg MPTP: 1.28 ± 0.06 ng/mg versus MPTP control: 0.93 ± 0.09 ng/mg). With regards to DOPAC levels, the 100 mg/kg fasudil group was significantly

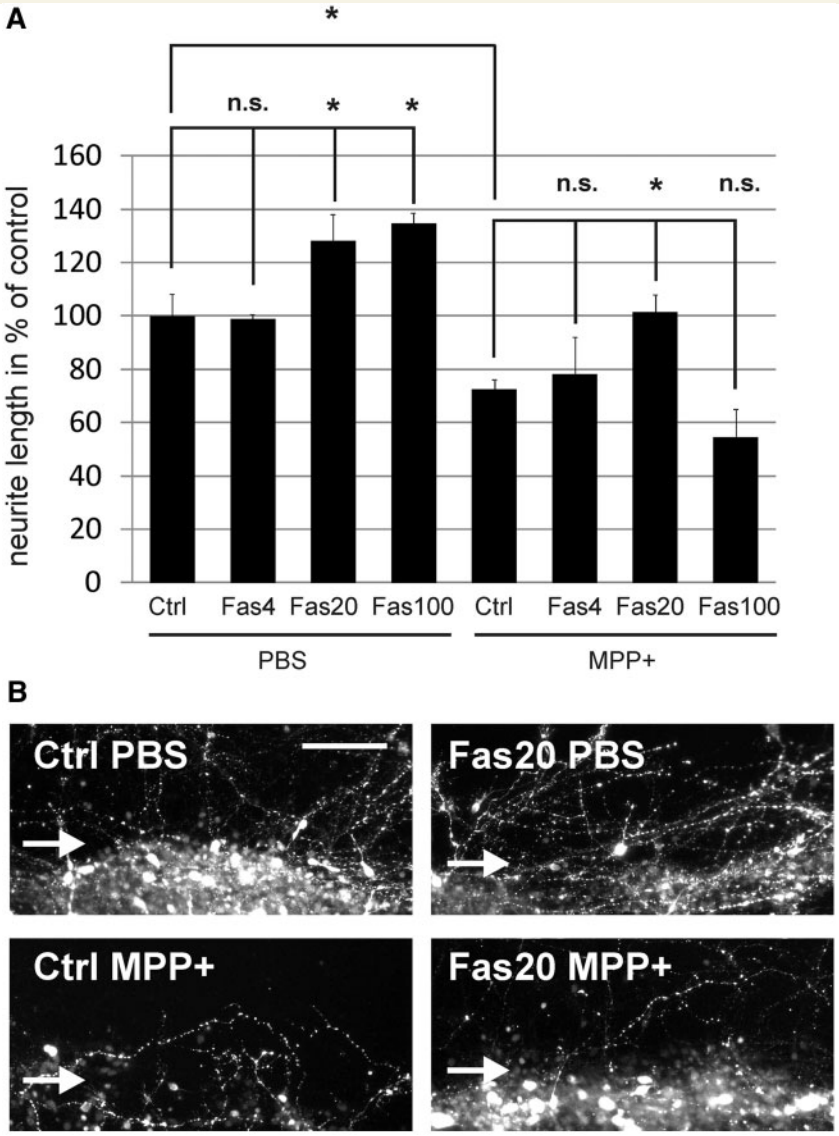

Figure 3 Neurite outgrowth of tyrosine hydroxylase-immunopositive cells from the lesion site 48 h after mechanical scratch with and without concomitant MPP^+ treatment. (**A**) MPP^+ (20 μM) toxicity leads to an overall reduction in neurite outgrowth. Supplementation with fasudil 20 μM (Fas20) results in an increased outgrowth both with PBS and with MPP^+ stress, whereas fasudil 100 μM (Fas100) does enhance neurite outgrowth only under PBS treatment. Bars represent means ± SEM. $*P < 0.05$, n.s = not significant. (**B**) Representative micrographs of midbrain dopaminergic neuron cultures labelled for tyrosine hydroxylase (white). Arrow indicates site of mechanical scratch lesion. Scale bar = 100 μm. Ctrl = control.

higher than the MPTP control group (2.35 ± 0.23 ng/mg), and there was only a trend towards higher dopamine levels (6.16 ± 0.81 ng/mg). Metabolite ratios were lower for both fasudil 30 mg/kg and for 100 mg/kg, however, without reaching significance (Fig. 7C–F).

Behavioural performance is improved by fasudil treatment

The neuroprotective effects of 2-week fasudil (100 mg/kg) treatment could also be visualized in a behavioural analysis of motor functions. The cylinder test evaluates sensorimotor coordination and forelimb use. It is often used to compare side differences in unilateral lesion models, but can also provide information about whole body coordination, which is best reflected in rears without any paw use. In the vehicle control group, rears against the cylinder wall with both paws were most frequent (67.2 ± 4.0%). Free rears were observed less often but still present to a considerable extent (26.8 ± 3.2%). Touches against the wall with either right (3.2 ± 1.5%) or left (2.8 ± 1.1%) paw were infrequent as was also shown for the other groups [MPTP control right (2.9 ± 1.0%), left (1.5 ± 0.7%); fasudil MPTP right (3.0 ± 1.0%), left (2.4 ± 0.8%)]. Animals that had been MPTP lesioned showed a significantly elevated ratio of wall touches with both paws (88.0 ± 1.9%) and significantly less free rears (7.7 ± 1.7%), indicating impaired coordination performance. The MPTP

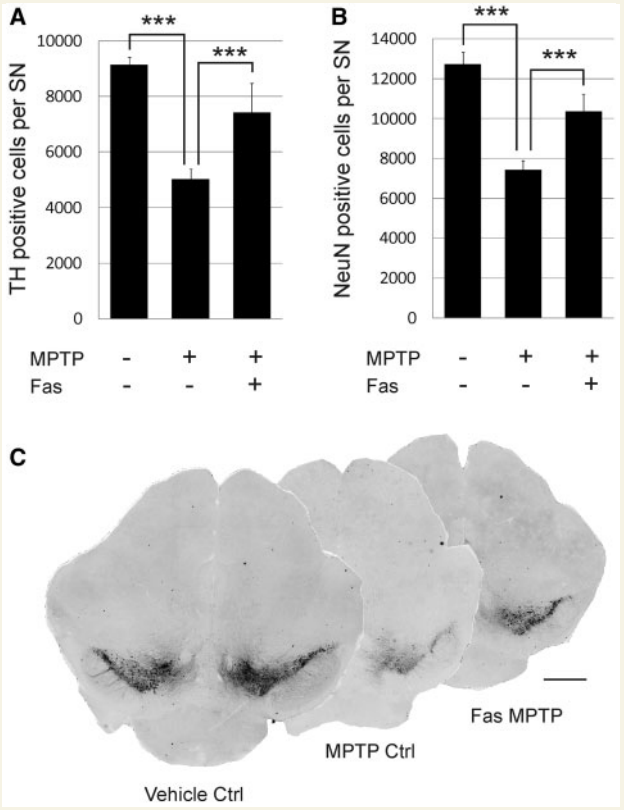

Figure 4 Nigral neuronal protection by 2 weeks rho kinase inhibition in MPTP-treated mice. (**A** and **B**) Quantification of nigral cells immunopositive for tyrosine hydroxylase (TH, **A**) or NeuN (**B**) in mice treated with vehicle (Vehicle Ctrl), MPTP and vehicle (MPTP Ctrl) or fasudil (100 mg/kg) and MPTP (Fas MPTP). (**C**) Representative micrographs of substantia nigra mouse brain sections labelled against tyrosine hydroxylase (black). Bars represent means ± SD. ***$P < 0.001$. Scale bar = 1 mm. Fas = fasudil; SN = substantia nigra.

group that had also received fasudil showed a behaviour that was similar to the non-MPTP-treated control group. Comparison with the MPTP lesion group indicated a significantly higher amount of free rears (16.5 ± 2.2%) and a reduced dependence of both paws touching the wall (78.1 ± 2.9%) (Fig. 8A). Another motor coordination test was included that evaluated average running performance on an accelerating rotarod. Here, the differences were less pronounced than in the cylinder test. Rotarod failure was earlier in the MPTP lesion group (143.2 ± 8.9 s) as in the vehicle control group (174.6 ± 11.4 s), and MPTP-treated animals that were also treated with fasudil showed a trend to longer time on the rotarod (163.8 ± 6.9 s), which was not significantly different from the vehicle control group (Fig. 8B).

The 6-week long-term treatment with fasudil 30 mg/kg or 100 mg/kg showed a maintained improvement of motor functions. In the cylinder test, the use of both paws was most common in the MPTP-lesioned control group (77.9 ± 5.4%), whereas a treatment with 30 mg/kg fasudil (49.0 ± 4.1%) or 100 mg/kg fasudil (59.2 ± 4.8%) reduced this behaviour in spite of the MPTP lesion. The more difficult free rears were observed more often in the 30 mg/kg fasudil group (39.8 ± 3.6%) than in the MPTP-lesioned control (19.8 ± 5.1%), whereas 100 mg/kg fasudil (34.3 ± 5.5%) did not result in a significant improvement (Fig. 9A). On the accelerated rotarod, MPTP-lesioned control animals did not show a difference in endurance (157.9 ± 9.8 s) compared with the vehicle control group (175.0 ± 12.8 s), and treatment with fasudil did not have a relevant influence on performance (fasudil 30 mg/kg: 149.8 ± 8.4 s; fasudil 100 mg/kg: 187.8 ± 9.4 s) (Fig. 9B).

Cellular survival after rho kinase inhibition is mediated through the Akt pathway

The molecular basis of the neuroprotective effect of fasudil was investigated in the MPP^+ intoxication paradigm of midbrain dopaminergic neurons *in vitro*. After 3 days in culture, cells were subjected to MPP^+ or vehicle treatment for 48 h. In this experiment, we additionally included Y-27632 to evaluate a possible group effect by comparing the neuroprotective potential of this alternative rho kinase inhibitor with fasudil in midbrain dopaminergic neurons. Both compounds were applied in optimal final concentrations based on previous studies (20 μM fasudil and 10 μM Y-27632). Analysing activation of the signal transducer and activator of transcription (STAT)3, Akt and MAPK cell survival pathways, we could detect only an activation of Akt as demonstrated by elevated phosphorylated Akt levels under MPP^+ lesioning conditions. This effect was significant in the fasudil group and showed a strong trend after application of Y-27632. Protein levels of Bcl2 and GAP43 were not changed (Fig. 10).

Discussion

Current medical treatment options for Parkinson's disease lack effectiveness in preventing clinical progression. Most experimental strategies have so far mainly focused on cellular conservation and neglected axonal protection, which may be a much earlier pharmacological target. We demonstrate in our preclinical study that pharmacological interference with rho kinase signalling is able to both preserve cellular and axonal function of lesioned dopaminergic cells. This is demonstrated both in the *in vitro* midbrain dopaminergic neuron MPP^+ paradigm and in the subchronic MPTP mouse model of Parkinson's disease *in vivo*.

Rho kinase inhibition protects from dopaminergic cell loss in toxicity-mediated lesion paradigms

Approaches that confer cellular protection in models of Parkinson's disease have been the focus of research in preclinical models of Parkinson's disease, as it was demonstrated that loss of dopaminergic cells is one of the major findings in post-mortem analysis of human patients with Parkinson's disease (reviewed in Dauer and Przedborski, 2003). Because MPTP models recapitulate dopaminergic cell loss, they are among the most frequently used toxin-based mouse models of Parkinson's disease in which cellular

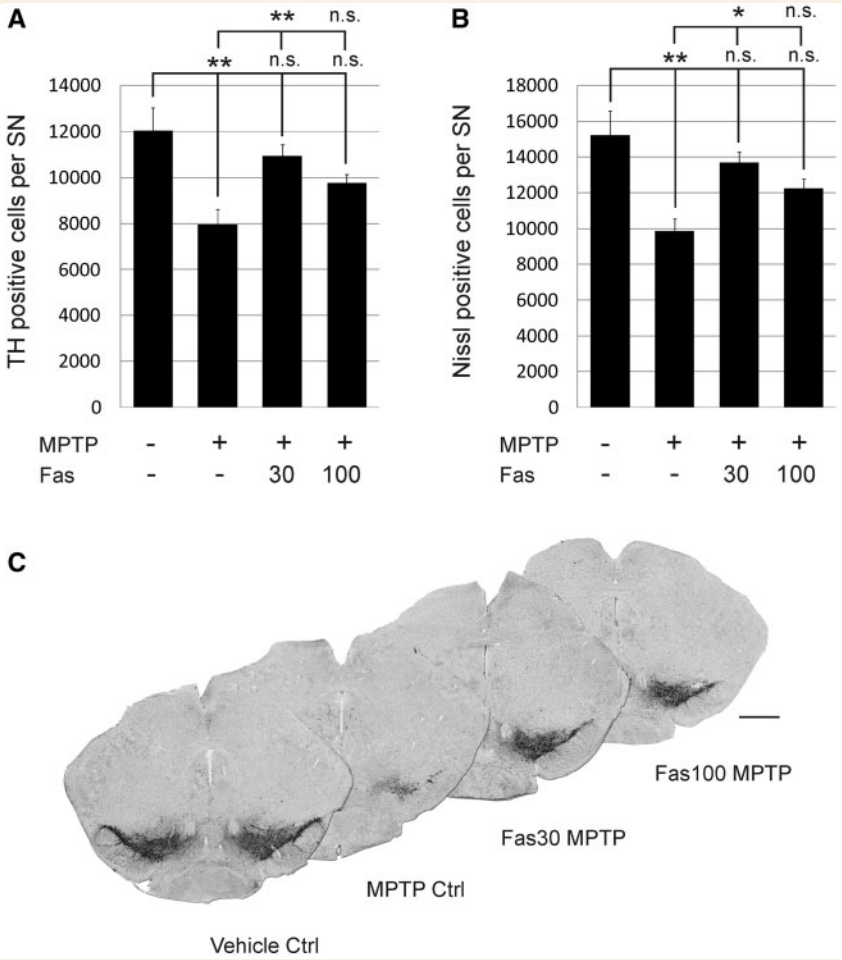

Figure 5 Nigral neuronal protection by 6 weeks rho kinase inhibition in MPTP-treated mice. (**A** and **B**) Quantification of nigral cells immunopositive for tyrosine hydroxylase (TH, **A**) or of Nissl-positive neurons (**B**) in mice treated with vehicle (Vehicle Ctrl), MPTP and vehicle (MPTP Ctrl), fasudil 30 mg/kg and MPTP (Fas30 MPTP) or fasudil 100 mg/kg and MPTP (Fas100 MPTP). (**C**) Representative micrographs of substantia nigra (SN) mouse brain sections labelled against tyrosine hydroxylase (black). Bars represent means ± SEM. $*P < 0.05$, $**P < 0.01$. n.s = not significant. Scale bar = 1 mm.

protective strategies have been examined. Nevertheless, only a few substances tested in these models have later been used in clinics, e.g. bromocriptine and pramipexole (Muralikrishnan and Mohanakumar, 1998; Zou *et al.*, 2000), which may be due to the fact that MPTP models replicate only a very selective part of Parkinson's disease pathology and do not model the largely unclear aetiological factors.

In our study, cultures of mouse ventral mesencephalon dopaminergic neurons were exposed to MPP^+ doses that resulted in cell death of more than one-third of the population of tyrosine hydroxylase-immunopositive cells. Pharmacological treatment with the rho kinase inhibitor fasudil was able to rescue more than half of the dying dopaminergic cells if optimal pharmacological concentrations were used (Fig. 1). High concentrations of fasudil most likely result in off-target effects and influence the function of other kinases, as has been demonstrated for protein kinase N1 (PKN1) and protein kinase C (PKC) (Davies *et al.*, 2000; Lingor *et al.*, 2007). For our *in vivo* studies, we used two different fasudil concentrations, 30 mg/kg and 100 mg/kg, which have been successfully used in previous preclinical studies (Abe *et al.*, 2004) and closely approach a human equivalent dose as calculated and applied for in clinical trials (Nohria *et al.*, 2006; Reagan-Shaw *et al.*, 2008). Based on these considerations, the neuroprotective potential of fasudil could also be shown in the MPTP model *in vivo* 2 and 6 weeks after initial MPTP lesion, where it attenuated nigral dopaminergic cell loss by >50% (Figs 4 and 5). This represents a robust protective effect compared with other therapeutically designed studies in this model (Nagel *et al.*, 2008; Frank *et al.*, 2012). Interestingly, the longer 6-week treatment with the fasudil dose of 30 mg/kg almost recovered tyrosine hydroxylase cell numbers to unlesioned control values, which indicates a sustained neuroprotective response over time, whereas fasudil 100 mg/kg showed only a trend to higher cell numbers. Our data therefore strongly suggest that fasudil, *in vitro* and *in vivo*, has a specific therapeutic dosage window where optimal neuroprotective effects can be expected.

Cellular protection mediated by pharmacological rho kinase inhibition has previously been demonstrated in other animal

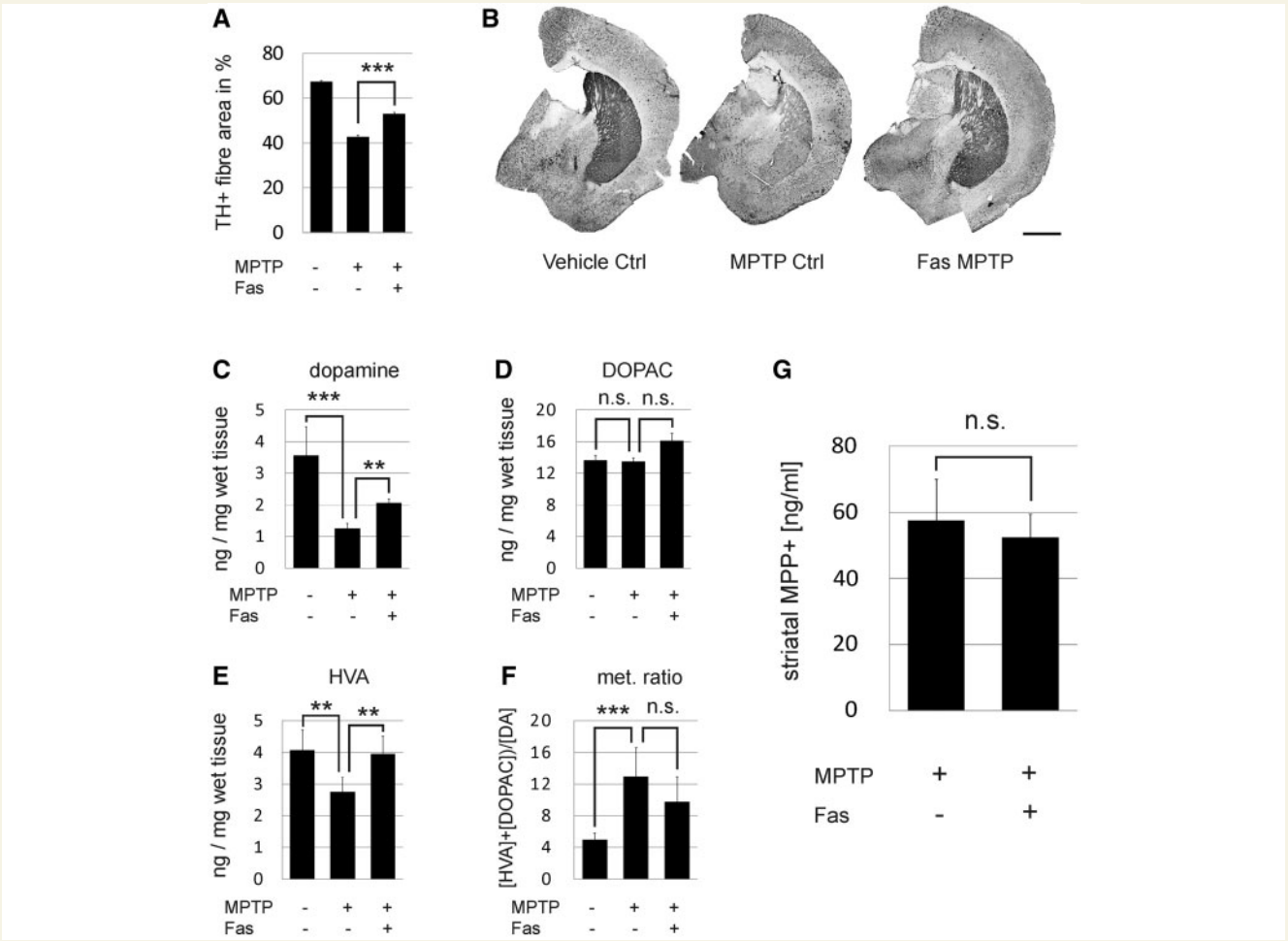

Figure 6 Striatal protection by 2 weeks rho kinase inhibition in MPTP-treated mice. (**A**) Quantification of striatal tyrosine hydroxylase-immunopositive fibre innervation in mice treated with vehicle (Vehicle Ctrl), MPTP and vehicle (MPTP Ctrl) or fasudil (100 mg/kg) and MPTP (Fas MPTP). (**B**) Representative micrographs of striatal fibres immunopositive for tyrosine hydroxylase (black). (**C–F**) HPLC analysis of striatal dopamine and its metabolites. (**G**) Striatal MPP^+ levels 90 min after MPTP injection. Bars represent means ± SEM. $^{**}P < 0.01$, $^{***}P < 0.001$. DOPAC = dihydroxyphenylacetic acid; HVA = homovanillic acid; met.ratio = metabolite ratio; n.s = not significant. Scale bar = 1 mm.

models. In a previous study, we were able to protect primary retinal ganglion cells from cell death induced by neurotrophin deprivation. Moreover, apoptotic cell death of axotomy-lesioned retinal ganglion cells *in vivo* was likewise reduced after intravitreal application of the rho kinase inhibitor Y-27632 (Lingor *et al.*, 2008). If serum-deprived organotypic retinal cell cultures were treated with the rho kinase inhibitor dimethylfasudil, a protection from apoptotic cell death could be achieved (Tura *et al.*, 2009). Interestingly, inflammatory processes were also attenuated in the latter study as was demonstrated by decreased levels of glial fibrillary acidic protein isoforms and reduced numbers of reactive astrocytes and microglia. The release of proinflammatory cytokines including tumour necrosis factor-α, interferon gamma and interleukin-6 was also shown to be reduced. Therefore, these parameters represent some of the most interesting targets for further analysis of fasudil-mediated neuroprotection in Parkinson's disease.

Neuroprotection by fasudil is mediated by activation of cell survival pathways

Neuroprotective survival cascades seem to be differentially activated under rho kinase inhibition. In an analysis of neuroprotective effects in neurotrophin-deprived retinal ganglion cells, we found that rho kinase inhibition with Y-27632 and concomitant treatment with CNTF leads to an increase in the activation of MAPK and Akt survival signalling pathways. However, this was not the case for STAT3 signalling that, although stimulated by ciliary neurotrophic factor (CNTF) alone, was attenuated in combination with Y-27632 (Lingor *et al.*, 2008). Evaluating cell survival responses after MPP^+ application in primary midbrain dopaminergic neurons, we observed that Akt signalling is significantly activated after rho kinase inhibition with fasudil being more effective than Y-27632 (Fig. 10). This is in line with data from other studies suggesting that Akt plays a crucial role for the integrity of

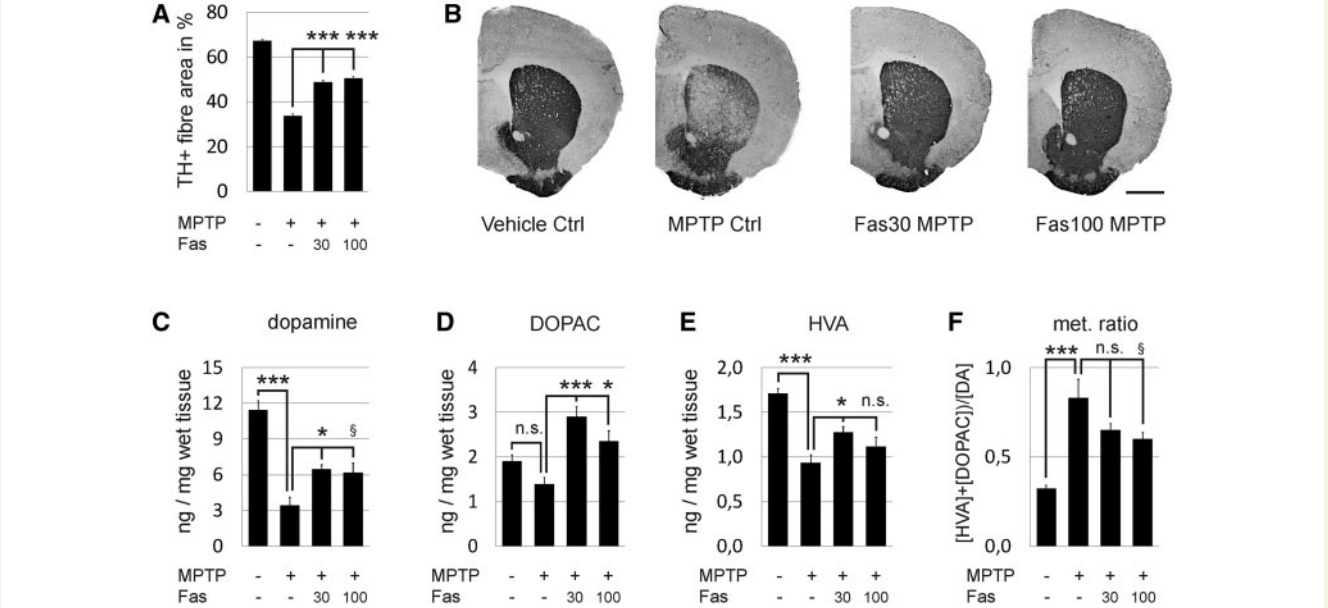

Figure 7 Striatal protection by 6 weeks rho kinase inhibition in MPTP-treated mice. (**A**) Quantification of striatal tyrosine hydroxylase-immunopositive fibre innervation in mice treated with vehicle (Vehicle Ctrl), MPTP and vehicle (MPTP Ctrl), fasudil 30 mg/kg and MPTP (Fas30 MPTP) or fasudil 100 mg/kg and MPTP (Fas100 MPTP). (**B**) Representative micrographs of striatal fibres immunopositive for tyrosine hydroxylase (TH, black). (**C–F**) HPLC analysis of striatal dopamine and its metabolites. Bars represent means ± SEM. $^{*}P < 0.05$, $^{***}P < 0.001$, $^{\S}P = 0.07$. DOPAC = Dihydroxyphenylacetic acid; HVA = homovanillic acid; n.s = not significant. Scale bar = 1 mm.

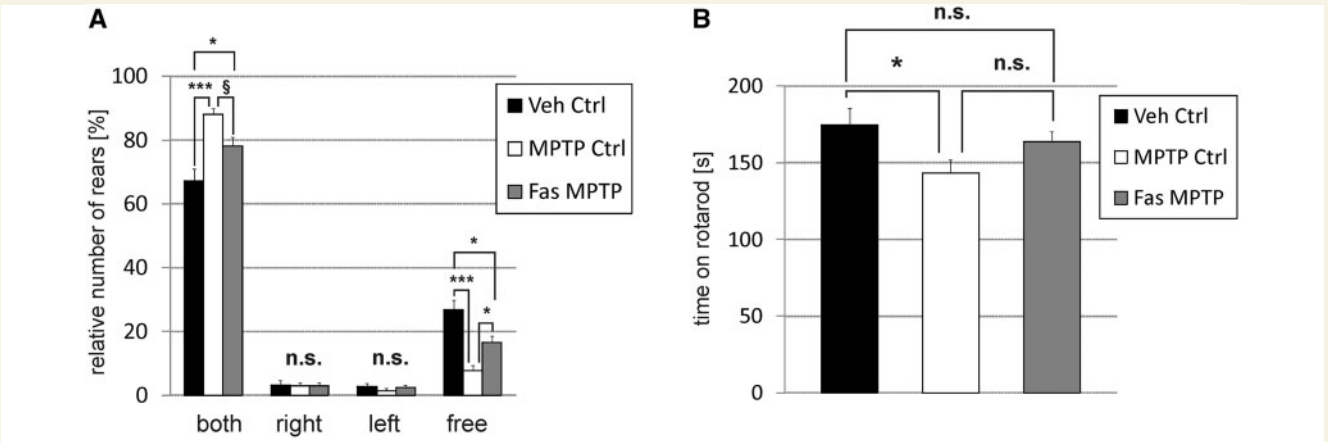

Figure 8 Behavioural analysis of mice treated with the rho kinase inhibitor fasudil for 2 weeks after the initial MPTP application. (**A**) Quantification of the percentage of rears against the wall with both paws, only right paw, only left paw or free rears. (**B**) Quantification of the average running time out of three runs on an accelerating rotarod. Bars represent means ± SEM. $^{*}P < 0.05$, $^{***}P < 0.001$, $^{\S}P = 0.06$. n.s = not significant.

dopaminergic neurons, as it induces various trophic effects in murine models of Parkinson's disease. The adeno-associated virus-assisted transduction of dopaminergic neurons in the substantia nigra with a gene encoding a myristoylated, constitutively active form of Akt resulted in pronounced trophic effects on dopamine neurons of adult and aged mice, including increases in neuron size, phenotypic markers and sprouting (Ries *et al.*, 2006). Moreover, striatal dopaminergic axons were significantly preserved due to suppression of axon degeneration in the 6-hydroxydopamine lesion mouse model of Parkinson's disease. This response has later been shown to be at least in part mediated by increased cellular mammalian target of rapamycin (mTor) activity and suppression of macroautophagy (Cheng *et al.*, 2011). If the transducing adeno-associated virus contained a dominant negative form of Akt, a decreased phenotypic expression of tyrosine hydroxylase was observed in striatal dopaminergic axons and terminals both in aged and in α-synuclein overexpressing mice (Kim *et al.*, 2011*a*). A putative downstream target of Akt is the Ras homolog enriched in brain/mammalian target of

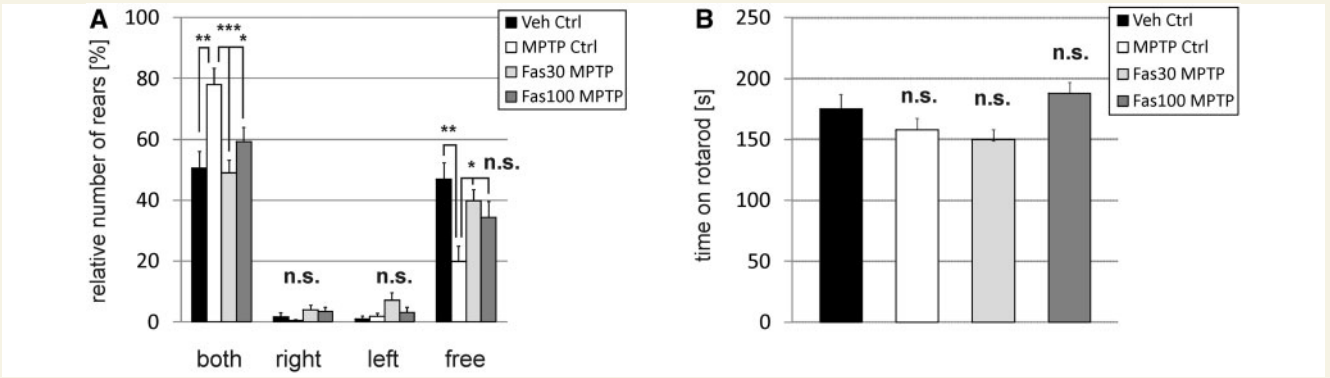

Figure 9 Behavioural analysis of mice treated with the rho kinase inhibitor fasudil for 6 weeks after the initial MPTP application. (**A**) Quantification of the percentage of rears against the wall with both paws, only right paw, only left paw or free rears. (**B**) Quantification of the average running time out of three runs on an accelerating rotarod. Bars represent means ± SEM. $*P < 0.05$, $**P < 0.01$, $***P < 0.001$. n.s = not significant.

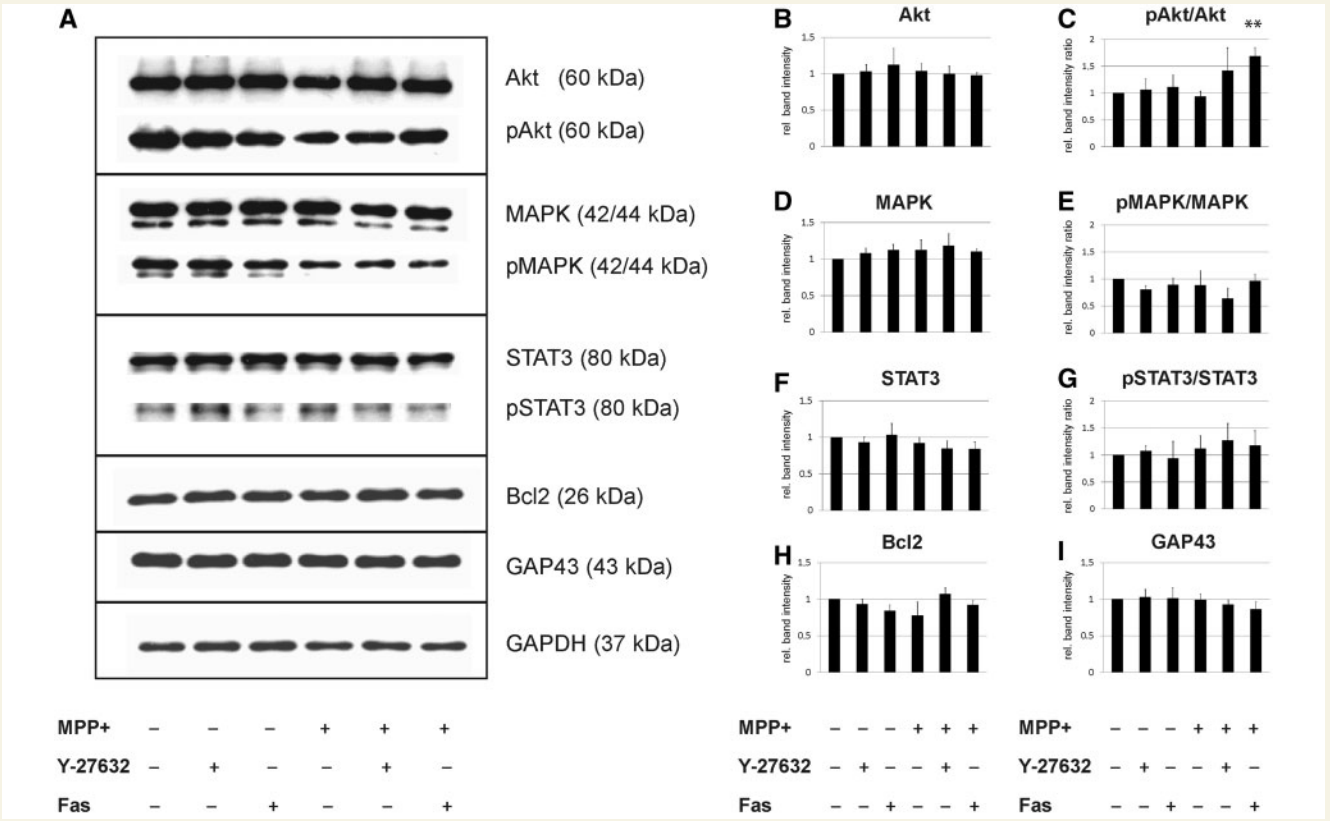

Figure 10 Activation of survival signalling pathways after rho kinase inhibition by fasudil 20 μM (Fas) or Y-27632 10 μM in midbrain dopaminergic neurons treated with or without MPP^+. (**A**) Representative immunoblots showing the regulation of Akt, pAkt, MAPK, pMAPK, STAT3, pSTAT3, Bcl2 and GAP43. (**B–I**) Quantification of immunoblot bands from three independent experiments for (total) Akt and phosphorylated Akt/(total) Akt (**B** and **C**), (total) MAPK and phosphorylated MAPK/(total) MAPK (**D** and **E**), (total) STAT3 and phosphorylated STAT3/(total) STAT3 (**F** and **G**), Bcl2 (**H**) and GAP43 (**I**). Bars represent means ± SEM. $**P < 0.01$.

rapamycin (Rheb/mTor) pathway, which can foster axon growth and halt nigral cell death following striatal 6-hydroxydopamine lesion upon activation by adeno-associated virus transduction of substania nigra neurons with constitutively active Rheb (Kim *et al.*, 2011*b*, 2012). The important role of Akt in Parkinson's disease pathology is also supported by the examination of human post-mortem Parkinson's disease brain dopaminergic neurons, which reveal a consistent depletion of phosphorylated Akt, but not of total Akt (Malagelada *et al.*, 2008).

Fasudil attenuates dopaminergic neurite degeneration, fosters neurite outgrowth and preserves dopaminergic striatal innervation

Next to perikaryal protection we were most interested in the potential of fasudil to protect neuritic and axonal structures after toxic lesion in our models. It has been demonstrated not only for PC-12 or Ntera-2 cells (Zhang *et al.*, 2006; Lingor *et al.*, 2007) but also for primary neurons that rho kinase inhibition fosters neurite outgrowth (Lehmann *et al.*, 1999; Borisoff *et al.*, 2003). Furthermore, rho kinase inhibition has also been attributed an axon-stabilizing function because it was able to protect from lesion-induced axon degeneration *in vitro*, supposedly being promoted by RhoA/rho kinase signalling (Gallo, 2004). In an analysis of the dopaminergic neurite network in culture, we found that an optimal concentration of 20 μM fasudil was able to completely prevent MPP^+-induced reduction of neurite length per cell. Under non-lesioning conditions, fasudil was even able to increase neurite length to >40% (Fig. 2A and C). When the entire neuritic network without normalization to cell numbers was quantified perikaryal survival effects elicited by fasudil additionally increase the cumulative, neurite length (Fig. 2B). Additionally, regenerative neurite outgrowth as evaluated in the scratch lesion model was significantly increased after fasudil treatment in an optimal dose range both in control and in MPP^+ stress conditions. Interestingly, the high concentration of fasudil 100 μM was able to increase the length of the longest neurites only under non-MPP^+ lesioning conditions, but failed if cells had been additionally subjected to MPP^+. This could be due to a toxic effect of the high fasudil dose in addition to the MPP^+ toxicity (Fig. 3). In view of all *in vitro* data, we conclude that fasudil is able to confer a strong perikaryal protection to dopaminergic neurons (Fig. 1). Furthermore, it has an additional, even more pronounced, protective effect on neuritic structures that is independent of perikaryal survival (Fig. 2). Similar to previous studies, fasudil reconfirmed its strong pro-regenerative properties (Fig. 3).

In the corresponding *in vivo* lesion models, the integrity of the striatal dopaminergic axonal terminal field was preserved by fasudil after MPTP treatment both morphologically and metabolically in the 2- and 6-week treatment paradigms (Figs 6 and 7). In contrast to the *in vitro* paradigm, a clear distinction between protection of perikarya and axons is more difficult to obtain, as both represent a functional entity. Treatment with fasudil conferred protection to perikarya and axons both in the 2- and 6-week evaluation. However, after 6-week treatment, when axonal pathology is strongest, fasudil (30 mg/kg) increased axonal structures by 44% whereas dopaminergic cells were increased by 38% only. This effect was also observed in the higher fasudil dose (100 mg/kg), which was less effective in protecting dopaminergic neurons after 6 weeks (23% increase of survival), whereas the striatal axon density was increased by 49%. These data suggest that the protective effect on dopaminergic striatal axons supercedes the pure neuroprotective effect of fasudil on dopaminergic neurons in the substantia nigra pars compacta. Concerning motor performance, fasudil 30 mg/kg best increased performance in the cylinder test, with almost reaching non-MPTP lesioned control values after 6 weeks (Figs 8 and 9). This indicates that there is an improvement of axonal terminal function with fasudil that is not evident in the axon structural analysis. Intriguingly, fasudil treatment showed a tendency towards increased striatal DOPAC levels after 2 weeks, and this effect was markedly significant after 6-week treatment (Figs 5 and 7). DOPAC is considered a primary intraneuronal metabolite of dopamine, whereas homovanillic acid rather represents a product of intra- and extraneuronal metabolism of released dopamine (Altar *et al.*, 1992), and this increase could speak in favour of a pro-regenerative effect of fasudil on remaining dopaminergic striatal fibres.

Conclusion

Our examination of pharmacological rho kinase inhibition in the MPP^+- and MPTP-based models of Parkinson's disease demonstrates that fasudil not only increased dopaminergic cell survival, but also protected the neuritic network *in vitro* and the striatal axonal innervation *in vivo*. This is of special pathophysiological relevance because degeneration of the neuronal soma and its processes has been demonstrated to use different molecular pathways, both of which seem to be beneficially influenced by rho kinase inhibition. Although numerous successful strategies to counteract cell death in models of neurodegenerative diseases have been proposed (Vila and Przedborski, 2003), simple cellular protection has not proven to be sufficient as a therapeutic option in the clinic (Olanow *et al.*, 2008). Rho kinase inhibitors such as fasudil may thus represent therapeutic agents that are dually effective in this context. Most importantly, fasudil has already been successfully implemented into clinical practice and is used in Japan for the treatment of patients suffering from subarachnoid haemorrhage-induced vasospasms due to its vasodilator effect on cerebral blood vessels (Zhao *et al.*, 2006). Its favourable safety profile may allow a reassessment of this drug and facilitate its evaluation in a pilot clinical study in patients with Parkinson's disease in the near future.

Acknowledgements

The authors thank Elisabeth Barski and Sabine Ceramella for expert technical assistance.

Funding

Michael J. Fox Foundation for Parkinson's Research (Target Validation Spring 2010 Program) (to P.L.); DFG Research Centre for Molecular Physiology of the Brain (CMPB), Göttingen, Germany (to P.L. and M.B.); Ernst-und-Berta-Grimmke-Stiftung (to L.T.).

Conflict of interest

None declared.

References

Abe K, Shimokawa H, Morikawa K, Uwatoku T, Oi K, Matsumoto Y, et al. Long-term treatment with a Rho-kinase inhibitor improves monocrotaline-induced fatal pulmonary hypertension in rats. Circ Res 2004; 94: 385–93.

Altar CA, Boylan CB, Jackson C, Hershenson S, Miller J, Wiegand SJ, et al. Brain-derived neurotrophic factor augments rotational behavior and nigrostriatal dopamine turnover in vivo. Proc Natl Acad Sci U S A 1992; 89: 11347–51.

Andringa G, Eshuis S, Perentes E, Maguire RP, Roth D, Ibrahim M, et al. TCH346 prevents motor symptoms and loss of striatal FDOPA uptake in bilaterally MPTP-treated primates. Neurobiol Dis 2003; 14: 205–17.

Beal MF, Matthews RT, Tieleman A, Shults CW. Coenzyme Q10 attenuates the 1-methyl-4-phenyl-1,2,3,tetrahydropyridine (MPTP) induced loss of striatal dopamine and dopaminergic axons in aged mice. Brain Res 1998; 783: 109–14.

Benazzouz A, Boraud T, Dubedat P, Boireau A, Stutzmann JM, Gross C. Riluzole prevents MPTP-induced parkinsonism in the rhesus monkey: a pilot study. Eur J Pharmacol 1995; 284: 299–307.

Bernheimer H, Birkmayer W, Hornykiewicz O, Jellinger K, Seitelberger F. Brain dopamine and the syndromes of Parkinson and Huntington. Clinical, morphological and neurochemical correlations. J Neurol Sci 1973; 20: 415–55.

Borisoff JF, Chan CC, Hiebert GW, Oschipok L, Robertson GS, Zamboni R, et al. Suppression of Rho-kinase activity promotes axonal growth on inhibitory CNS substrates. Mol Cell Neurosci 2003; 22: 405–16.

Braak H, Del Tredici K, Rub U, de Vos RA, Jansen Steur EN, Braak E. Staging of brain pathology related to sporadic Parkinson's disease. Neurobiol Aging 2003; 24: 197–211.

Burke RE. Intracellular signalling pathways in dopamine cell death and axonal degeneration. Prog Brain Res 2010; 183: 79–97.

Burke RE, O'Malley K. Axon degeneration in Parkinson's disease. Exp Neurol 2012; [Epub ahead of print].

Cannon JR, Greenamyre JT. Neurotoxic in vivo models of Parkinson's disease recent advances. Prog Brain Res 2010; 184: 17–33.

Cheng HC, Ulane CM, Burke RE. Clinical progression in Parkinson disease and the neurobiology of axons. Ann Neurol 2010; 67: 715–25.

Cheng HC, Kim SR, Oo TF, Kareva T, Yarygina O, Rzhetskaya M, et al. Akt suppresses retrograde degeneration of dopaminergic axons by inhibition of macroautophagy. J Neurosci 2011; 31: 2125–35.

Coleman M. Axon degeneration mechanisms: commonality amid diversity. Nat Rev Neurosci 2005; 6: 889–98.

Coleman MP, Perry VH. Axon pathology in neurological disease: a neglected therapeutic target. Trends Neurosci 2002; 25: 532–7.

Dauer W, Przedborski S. Parkinson's disease: mechanisms and models. Neuron 2003; 39: 889–909.

Davies SP, Reddy H, Caivano M, Cohen P. Specificity and mechanism of action of some commonly used protein kinase inhibitors. Biochem J 2000; 351: 95–105.

Dehmer T, Heneka MT, Sastre M, Dichgans J, Schulz JB. Protection by pioglitazone in the MPTP model of Parkinson's disease correlates with I kappa B alpha induction and block of NF kappa B and iNOS activation. J Neurochem 2004; 88: 494–501.

Frank T, Klinker F, Falkenburger BH, Laage R, Luhder F, Goricke B, et al. Pegylated granulocyte colony-stimulating factor conveys long-term neuroprotection and improves functional outcome in a model of Parkinson's disease. Brain 2012; 135: 1914–25.

Gallo G. Myosin II activity is required for severing-induced axon retraction in vitro. Exp Neurol 2004; 189: 112–21.

Greggio E, Cookson MR. Leucine-rich repeat kinase 2 mutations and Parkinson's disease: three questions. ASN Neuro 2009. 1 pii: e00002.

Hashimoto R, Nakamura Y, Kosako H, Amano M, Kaibuchi K, Inagaki M, et al. Distribution of Rho-kinase in the bovine brain. Biochem Biophys Res Commun 1999; 263: 575–9.

Herkenham M, Little MD, Bankiewicz K, Yang SC, Markey SP, Johannessen JN. Selective retention of MPP+ within the monoaminergic systems of the primate brain following MPTP administration: an in vivo autoradiographic study. Neuroscience 1991; 40: 133–58.

Kim SR, Ries V, Cheng HC, Kareva T, Oo TF, Yu WH, et al. Age and alpha-synuclein expression interact to reveal a dependence of dopaminergic axons on endogenous Akt/PKB signaling. Neurobiol Dis 2011a; 44: 215–22.

Kim SR, Chen X, Oo TF, Kareva T, Yarygina O, Wang C, et al. Dopaminergic pathway reconstruction by Akt/Rheb-induced axon regeneration. Ann Neurol 2011b; 70: 110–20.

Kim SR, Kareva T, Yarygina O, Kholodilov N, Burke RE. AAV transduction of dopamine neurons with constitutively active Rheb protects from neurodegeneration and mediates axon regrowth. Mol Ther 2012; 20: 275–86.

Komagome R, Kimura K, Saito M. Postnatal changes in Rho and Rho-related proteins in the mouse brain. Jpn J Vet Res 2000; 47: 127–33.

Kramer ML, Schulz-Schaeffer WJ. Presynaptic alpha-synuclein aggregates, not Lewy bodies, cause neurodegeneration in dementia with Lewy bodies. J Neurosci 2007; 27: 1405–10.

Lang AE. Neuroprotection in Parkinson's disease: and now for something completely different? Lancet Neurol 2006; 5: 990–1.

Langston JW, Ballard P, Tetrud JW, Irwin I. Chronic Parkinsonism in humans due to a product of meperidine-analog synthesis. Science 1983; 219: 979–80.

Lees AJ, Hardy J, Revesz T. Parkinson's disease. Lancet 2009; 373: 2055–66.

Lehmann M, Fournier A, Selles-Navarro I, Dergham P, Sebok A, Leclerc N, et al. Inactivation of Rho signaling pathway promotes CNS axon regeneration. J Neurosci 1999; 19: 7537–47.

Li LH, Qin HZ, Wang JL, Wang J, Wang XL, Gao GD. Axonal degeneration of nigra-striatum dopaminergic neurons induced by 1-methyl-4-phenyl-1,2,3,6-tetrahydropyridine in mice. J Int Med Res 2009; 37: 455–63.

Lingor P, Unsicker K, Krieglstein K. Midbrain dopaminergic neurons are protected from radical induced damage by GDF-5 application. Short communication. J Neural Transm 1999; 106: 139–44.

Lingor P, Teusch N, Schwarz K, Mueller R, Mack H, Bahr M, et al. Inhibition of Rho kinase (ROCK) increases neurite outgrowth on chondroitin sulphate proteoglycan in vitro and axonal regeneration in the adult optic nerve in vivo. J Neurochem 2007; 103: 181–9.

Lingor P, Tonges L, Pieper N, Bermel C, Barski E, Planchamp V, et al. ROCK inhibition and CNTF interact on intrinsic signalling pathways and differentially regulate survival and regeneration in retinal ganglion cells. Brain 2008; 131: 250–63.

Lingor P, Liman J, Kallenberg K, Sahlmann CO, Bähr M. Rana A, editor. Parkinson's Disease / Book 1. Vienna: InTech Open Access Company; 2011.

Loirand G, Pacaud P. The role of Rho protein signaling in hypertension. Nat Rev Cardiol 2010; 7: 637–47.

Malagelada C, Jin ZH, Greene LA. RTP801 is induced in Parkinson's disease and mediates neuron death by inhibiting Akt phosphorylation/activation. J Neurosci 2008; 28: 14363–71.

Mueller BK, Mack H, Teusch N. Rho kinase, a promising drug target for neurological disorders. Nat Rev Drug Discov 2005; 4: 387–98.

Muralikrishnan D, Mohanakumar KP. Neuroprotection by bromocriptine against 1-methyl-4-phenyl-1,2,3,6-tetrahydropyridine-induced neurotoxicity in mice. FASEB J 1998; 12: 905–12.

Muroyama A, Kobayashi S, Mitsumoto Y. Loss of striatal dopaminergic terminals during the early stage in response to MPTP injection in C57BL/6 mice. Neurosci Res 2011; 69: 352–5.

Nagel F, Falkenburger BH, Tonges L, Kowsky S, Poppelmeyer C, Schulz JB, et al. Tat-Hsp70 protects dopaminergic neurons in midbrain cultures and in the substantia nigra in models of Parkinson's disease. J Neurochem 2008; 105: 853–64.

Nohria A, Grunert ME, Rikitake Y, Noma K, Prsic A, Ganz P, et al. Rho kinase inhibition improves endothelial function in human subjects with coronary artery disease. Circ Res 2006; 99: 1426–32.

Olanow CW, Schapira AH, LeWitt PA, Kieburtz K, Sauer D, Olivieri G, et al. TCH346 as a neuroprotective drug in Parkinson's disease: a double-blind, randomised, controlled trial. Lancet Neurol 2006; 5: 1013–20.

Olanow CW, Kieburtz K, Schapira AH. Why have we failed to achieve neuroprotection in Parkinson's disease? Ann Neurol 2008; 64 (Suppl 2): S101–10.

Perry TL, Yong VW, Clavier RM, Jones K, Wright JM, Foulks JG, et al. Partial protection from the dopaminergic neurotoxin N-methyl-4-phenyl-1,2,3,6-tetrahydropyridine by four different antioxidants in the mouse. Neurosci Lett 1985; 60: 109–14.

Przedborski S, Jackson-Lewis V, Yokoyama R, Shibata T, Dawson VL, Dawson TM. Role of neuronal nitric oxide in 1-methyl-4-phenyl-1,2,3,6-tetrahydropyridine (MPTP)-induced dopaminergic neurotoxicity. Proc Natl Acad Sci U S A 1996; 93: 4565–71.

Przedborski S, Jackson-Lewis V, Naini AB, Jakowec M, Petzinger G, Miller R, et al. The parkinsonian toxin 1-methyl-4-phenyl-1,2,3,6-tetrahydropyridine (MPTP): a technical review of its utility and safety. J Neurochem 2001; 76: 1265–74.

Raff MC, Whitmore AV, Finn JT. Axonal self-destruction and neurodegeneration. Science 2002; 296: 868–71.

Reagan-Shaw S, Nihal M, Ahmad N. Dose translation from animal to human studies revisited. FASEB J 2008; 22: 659–61.

Ries V, Henchcliffe C, Kareva T, Rzhetskaya M, Bland R, During MJ, et al. Oncoprotein Akt/PKB induces trophic effects in murine models of Parkinson's disease. Proc Natl Acad Sci U S A 2006; 103: 18757–62.

Saporito MS, Brown EM, Miller MS, Carswell S. CEP-1347/KT-7515, an inhibitor of c-jun N-terminal kinase activation, attenuates the 1-methyl-4-phenyl tetrahydropyridine-mediated loss of nigrostriatal dopaminergic neurons in vivo. J Pharmacol Exp Ther 1999; 288: 421–7.

Schallert T, Fleming SM, Leasure JL, Tillerson JL, Bland ST. CNS plasticity and assessment of forelimb sensorimotor outcome in unilateral rat models of stroke, cortical ablation, parkinsonism and spinal cord injury. Neuropharmacology 2000; 39: 777–87.

Schulz JB, Henshaw DR, Matthews RT, Beal MF. Coenzyme Q10 and nicotinamide and a free radical spin trap protect against MPTP neurotoxicity. Exp Neurol 1995; 132: 279–83.

Storch A, Jost WH, Vieregge P, Spiegel J, Greulich W, Durner J, et al. Randomized, double-blind, placebo-controlled trial on symptomatic effects of coenzyme Q(10) in Parkinson disease. Arch Neurol 2007; 64: 938–44.

Strickland D, Bertoni JM. Parkinson's prevalence estimated by a state registry. Mov Disord 2004; 19: 318–23.

Szego EM, Gerhardt E, Kermer P, Schulz JB. A30P alpha-synuclein impairs dopaminergic fiber regeneration and interacts with L-DOPA replacement in MPTP-treated mice. Neurobiol Dis 2012; 45: 591–600.

Tonges L, Planchamp V, Koch JC, Herdegen T, Bahr M, Lingor P. JNK isoforms differentially regulate neurite growth and regeneration in dopaminergic neurons in vitro. J Mol Neurosci 2011a; 45: 284–93.

Tonges L, Koch JC, Bahr M, Lingor P. ROCKing regeneration: rho kinase inhibition as molecular target for neurorestoration. Front Mol Neurosci 2011b; 4: 39.

Tura A, Schuettauf F, Monnier PP, Bartz-Schmidt KU, Henke-Fahle S. Efficacy of Rho-kinase inhibition in promoting cell survival and reducing reactive gliosis in the rodent retina. Invest Ophthalmol Vis Sci 2009; 50: 452–61.

Vila M, Przedborski S. Targeting programmed cell death in neurodegenerative diseases. Nat Rev Neurosci 2003; 4: 365–75.

Volpicelli-Daley LA, Luk KC, Patel TP, Tanik SA, Riddle DM, Stieber A, et al. Exogenous alpha-synuclein fibrils induce Lewy body pathology leading to synaptic dysfunction and neuron death. Neuron 2011; 72: 57–71.

Wu DC, Teismann P, Tieu K, Vila M, Jackson-Lewis V, Ischiropoulos H, et al. NADPH oxidase mediates oxidative stress in the 1-methyl-4-phenyl-1,2,3,6-tetrahydropyridine model of Parkinson's disease. Proc Natl Acad Sci U S A 2003; 100: 6145–50.

Zhang Z, Ottens AK, Larner SF, Kobeissy FH, Williams ML, Hayes RL, et al. Direct Rho-associated kinase inhibition [correction of inhibition] induces cofilin dephosphorylation and neurite outgrowth in PC-12 cells. Cell Mol Biol Lett 2006; 11: 12–29.

Zhao J, Zhou D, Guo J, Ren Z, Zhou L, Wang S, et al. Effect of fasudil hydrochloride, a protein kinase inhibitor, on cerebral vasospasm and delayed cerebral ischemic symptoms after aneurysmal subarachnoid hemorrhage. Neurol Med Chir (Tokyo) 2006; 46: 421–8.

Zou L, Xu J, Jankovic J, He Y, Appel SH, Le W. Pramipexole inhibits lipid peroxidation and reduces injury in the substantia nigra induced by the dopaminergic neurotoxin 1-methyl-4-phenyl-1,2,3,6-tetrahydropyridine in C57BL/6 mice. Neurosci Lett 2000; 281: 167–70.